Article

Deracemization of a Dynamic Combinatorial Library Induced by (#)-Cytidine and (#)-2-Thiocytidine

Mee-Kyung Chung, Christine M. Hebling, James W. Jorgenson, Kay Severin, Stephen J. Lee, and Michel R. Gagne#

J. Am. Chem. Soc., **2008**, 130 (35), 11819-11827 • DOI: 10.1021/ja803658n • Publication Date (Web): 09 August 2008

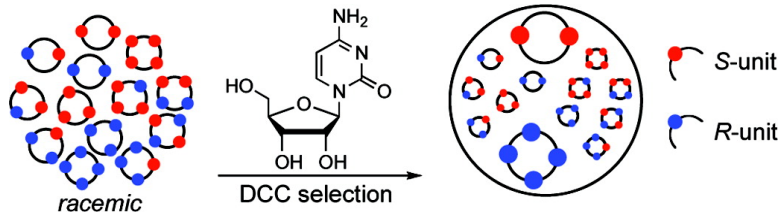

More About This Article

Additional resources and features associated with this article are available within the HTML version:

- Supporting Information
- Access to high resolution figures
- Links to articles and content related to this article
- Copyright permission to reproduce figures and/or text from this article

View the Full Text HTML

J|A|C|S
ARTICLES

Published on Web 08/09/2008

Deracemization of a Dynamic Combinatorial Library Induced by (−)-Cytidine and (−)-2-Thiocytidine

Mee-Kyung Chung,[§] Christine M. Hebling,[§] James W. Jorgenson,[§] Kay Severin,[†] Stephen J. Lee,[‡] and Michel R. Gagné*,[§]

Department of Chemistry, University of North Carolina at Chapel Hill, Chapel Hill, North Carolina 27599-3290, Institut des Sciences et Ingénieries Chimiques, École Polytechnique Fédérale de Lausanne, 1015 Lausanne, Switzerland, and U.S. Army Research Office, P.O. Box 12211, Research Triangle Park, North Carolina 27709

Received May 22, 2008; E-mail: mgagne@unc.edu

Abstract: A dynamic combinatorial library composed of racemic hydrazone-based dipeptides becomes deracemized on binding to the chiral analytes (−)-cytidine and (−)-2-thiocytidine through the amplification of two receptors, (*SS*)-dimer and (*RRRR*)-tetramer. The deracemization phenomenon was investigated by laser polarimetry, mass-tagged pseudo-enantiomers in conjunction with electrospray ionization mass spectrometry, HPLC/UV-MS, UPLC/UV-MS, rapid-resolution LC-MS, collision-induced dissociation MS/MS, and numerical simulations. These data were consistent with a phenomenon where (*SS*)-dimer and (*RRRR*)-tetramer selectively bind the chiral analyte in preference to their enantiomeric counterparts, which ultimately causes them to be amplified and the library to become deracemized.

Introduction

Dynamic combinatorial chemistry (DCC) has developed into a powerful tool for identifying new host−guest combinations by equilibrium perturbation.[1] Despite the many successes, however, few DCC experiments have been reported with the intention of finding *enantioselective* receptors, though numerous cases of *diastereoselective* receptor amplification using achiral guests from chiral dynamic combinatorial libraries (DCLs) and distinct cyclomer amplifications for diastereomeric guests have been observed.[2] Recently, Sanders reported that different diastereoisomers of a guest elicit unique receptors (dimers and tetramers) from an enantiopure DCC library.[3] A DCC resolution of a dynamic nitroaldol library coupled to a secondary enzyme mediated kinetic resolution is also known.[4]

Previously, we demonstrated that an enantioselective receptor for (−)-adenosine could be discovered from a *racemic* cyclic hydrazone family of DCC dipeptides by the use of (a) laser polarimetry (LP) detection coupled with HPLC and (b) pseudo-enantiomers to detect the enantio-imbalance caused by the stereoselective host−guest binding.[5] In subsequent research, we have discovered a unique scenario wherein the addition of (−)-cytidine or (−)-2-thiocytidine caused the initially racemic library to reach its global energy minimum by *deracemizing*. The process of transforming a racemate into enantiopure products is of considerable interest, and current methods include dynamic kinetic resolutions, kinetic asymmetric transformations, and stereoinversions.[6,7] The deracemization of a racemic DCL by a guest-induced thermodynamic perturbation is unusual and, to our knowledge, unprecedented. We show herein that this phenomenon is a result of in situ generation and amplification

[§] University of North Carolina at Chapel Hill.
[†] École Polytechnique Fédérale de Lausanne (EPFL).
[‡] U.S. Army Research Office.

(1) For reviews, see: (a) Ladame, S. *Org. Biomol. Chem.* **2008**, *6*, 219–226. (b) Ludlow, R. F.; Otto, S. *Chem. Soc. Rev.* **2008**, *37*, 101–108. (c) Lehn, J.-M. *Chem. Soc. Rev.* **2007**, *36*, 151–160. (d) Corbett, P. T.; Leclaire, J.; Vial, L.; West, K. R.; Wietor, J.-L.; Sanders, J. K. M.; Otto, S. *Chem. Rev.* **2006**, *106*, 3652–3711. (e) Zhang, W.; Moore, J. S. *Angew. Chem., Int. Ed.* **2006**, *45*, 4416–4439. (f) Sanders, J. K. M. *Philos. Trans. R. Soc. A* **2004**, *362*, 1239–1245. (g) Ramstrom, O.; Lehn, J.-M. *Nat. Rev. Drug Discovery* **2002**, *1*, 26–36. (h) Otto, S.; Furlan, R. L. E.; Sanders, J. K. M. *Drug Discovery Today* **2002**, *7*, 117–125.

(2) (a) González-Álvarez, A.; Alfonso, I.; Gotor, V. *Chem. Commun.* **2006**, 2224–2226. (b) Lam, R. T. S.; Belenguer, A.; Roberts, S. L.; Naumann, C.; Jarrosson, T.; Otto, S.; Sanders, J. K. M. *Science* **2005**, *308*, 667–669. (c) Corbett, P. T.; Tong, L. H.; Sanders, J. K. M.; Otto, S. *J. Am. Chem. Soc.* **2005**, *127*, 8902–8903. (d) ten Cate, A. T.; Dankers, P. Y. W.; Sijbesma, R. P.; Meijer, E. W. *J. Org. Chem.* **2005**, *70*, 5799–5803. (e) Telfer, S. G.; Yang, X.-J.; Williams, A. F. *J. Chem. Soc., Dalton Trans.* **2004**, 699–705.

(3) Bulos, F.; Robert, S. L.; Furlan, R. L. E.; Sanders, J. K. M. *Chem. Commun.* **2007**, 3092–3093.

(4) Vongvilai, P.; Angelin, M.; Larsson, R.; Ramström, O. *Angew. Chem., Int. Ed.* **2007**, *46*, 948–950.

(5) Voshell, S. M.; Lee, S. J.; Gagné, M. R. *J. Am. Chem. Soc.* **2006**, *128*, 12422–12423.

(6) Kinetic and thermodynamic resolutions continue to be an active field of endeavor. For several recent reviews on this broad topic, see: (a) Blacker, A. J.; Stirling, M. J.; Page, M. I. *Org. Process Res. Dev.* **2007**, *11*, 642–648. (b) Gruber, C. C.; Lavandera, I.; Faber, K.; Kroutil, W. *Adv. Synth. Catal.* **2006**, *348*, 1789–1850. (c) Fisher, H. F. *Acc. Chem. Res.* **2005**, *38*, 157–166. (d) Dehli, J. R.; Gotor, V. *Chem. Soc. Rev.* **2002**, *31*, 365–370. (e) Huerta, F. F.; Minidis, A. B. E.; Bäckvall, J.-E. *Chem. Soc. Rev.* **2001**, *30*, 321–331. (f) Faber, K. *Chem. Eur. J.* **2001**, *7*, 5005–5010. (g) Beak, P.; Anderson, D. R.; Curtis, M. D.; Laumer, J. M.; Pippel, D. J.; Weisenburger, G. A. *Acc. Chem. Res.* **2000**, *33*, 715–727. (h) Caddick, S.; Jenkins, K. *Chem. Soc. Rev.* **1996**, *25*, 447–456.

(7) For a recent self-sorting of a racemic metal-template host-guest assembly, see: Hutin, M.; Cramer, C. J.; Gagliardi, L.; Shahi, A. R. M.; Bernardinelli, G.; Cerny, R.; Nitschke, J. R. *J. Am. Chem. Soc.* **2007**, *129*, 8774–8780.

of two receptors for (−)-cytidine or (−)-2-thiocytidine and that each is constructed of enantiomeric building blocks.

Experimental Section

General Methods. Chemicals were purchased from Aldrich and used as received. Anhydrous acetonitrile was purchased from Acros. Acetone-d_6 was purchased from Cambridge Isotope Laboratory, Inc. NMR spectra were recorded on a Bruker Avance 400 spectrometer. High-performance liquid chromatography (HPLC) analysis was performed on a Hewlett-Packard Series 1100 instrument, using an Agilent Eclipse XDB-C18 column (4.6 × 150 mm, 4.6 μm) with gradient elution (methanol/acetonitrile/water) at a flow rate of 1.0 mL/min (column at room temperature). The injection volume for a 5 mM DCL was typically 10 μL. UV absorbance chromatograms were recorded at wavelengths of 220 and 289 nm. The laser polarimeter signal was recorded with a PDR-Chiral, Inc. advanced laser polarimeter equipped with a 3.5 mW laser diode system (670 nm) and an 18 μL flow cell. The data were analyzed using the HP Chemstation software. Ultra-performance liquid chromatography (UPLC)-MS analysis was performed on a Waters Acquity UPLC instrument, using an Acquity UPLC BEH C18 column (2.1 × 100 mm, 1.7 μm) with various gradient elution (17 to 30% acetonitrile/water containing 0.2% formic acid, in 12.5 min) at a flow rate of either 0.3 mL/min (column temperature, 29 °C) or 0.7 mL/min (column temperature, 55 °C). The injection volume for a 5 mM DCL was typically 1.5 μL. The eluent was analyzed by a Waters Micromass ZQ mass spectrometer in positive ion mode with the electrospray ionization (ESI) source. Rapid-resolution LC-MS analysis was performed on an Agilent Series 1200 instrument, using an Agilent Zorbax Eclipse XDB-C18 column (4.6 × 50 mm, 1.8 μm) with gradient elution (acetonitrile/water containing 0.2% formic acid, in 13 min) at a flow rate of 1.8 mL/min (gradient column temperature, 50 to 45 °C). The injection volume for a 5 mM DCL was typically 1.2 μL. The eluent was analyzed by an Agilent 6100 series LC/MSD Quadrupole SL mass spectrometer in positive ion mode with the ESI source.

Generation of DCLs Using (*rac*)-1. (*rac*)-**1** was prepared using a literature method.[5] For LC analysis, 5 mM DCLs were prepared on a 1 mL scale. (*rac*)-**1** (9.8 mg, 25 μmol) was dissolved in anhydrous acetonitrile (5 mL), and trifluoroacetic acid (TFA; 50 equiv, 1250 μmol, 93 μL) was added. Aliquots of this solution (1.0 mL) were transferred to two vials [an empty vial and a vial containing a template: (−)-adenosine (13.4 mg, 50 μmol), (−)-cytidine (12.2 mg, 50 μmol), and (−)-2-thiocytidine (13.0 mg, 50 μmol)]. The solutions were allowed to sit overnight (12−16 h), during which time a steady state was reached for the untemplated DCL prior to LC analyses.

Generation of a Racemic DCL from (*S*)-1-d_6 and (*R*)-1. α-Methylalanine-d_6[8] was synthesized following a previously reported procedure from acetone-d_6. ^{1}H NMR and MS analysis showed that ca. 95% of the α-Me protons were deuterated. (*S*)-**1**-d_6 and (*R*)-**1** were prepared in procedures analogous to that used for (*rac*)-**1**. For UPLC-MS and rapid-resolution LC-MS analyses, 5 mM DCLs were prepared on a 1 mL scale. (*S*)-**1**-d_6 (19.9 mg, 50 μmol) was dissolved in 10 mL of anhydrous acetonitrile. (*R*)-**1** (19.6 mg, 50 μmol) was dissolved in 10 mL of anhydrous acetonitrile. A 2.5 mL portion of the (*S*)-**1**-d_6 solution was mixed with 2.5 mL of the (*R*)-**1** solution. TFA (50 equiv, 1250 μmol, 93 μL) was added to the resultant solution. Aliquots of this solution (1.0 mL) were transferred to two vials (an empty vial and a vial containing a template). The solutions were allowed to sit overnight (12−16 h) during which the steady state was reached for untemplated DCL before various LC-MS analyses.

Generation of Enantiopure DCLs Using (*S*)-1 and (*R*)-1. (*S*)-**1** and (*R*)-**1** were prepared using the same synthetic procedure as that for (*rac*)-**1**. Five millimolar DCLs were prepared on a 1 mL scale. (*S*)-**1** or (*R*)-**1** (9.8 mg, 25 μmol) was dissolved in anhydrous acetonitrile (5 mL), and TFA (50 equiv, 1250 μmol, 93 μL) was added. Aliquots of this solution (1.0 mL) were transferred to two vials (an empty vial and a vial containing a template). The solutions were allowed to sit overnight (12−16 h), during which the steady state was reached for the untemplated DCL prior to various LC analyses.

Scheme 1

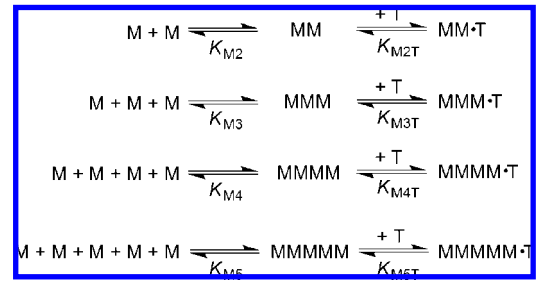

Generation of Enantiopure (*S*)- and (*R*)-DCLs for Simulations. A series of DCLs were prepared on a 1 mL scale using (*S*)-**1** or (*R*)-**1** (5 mM in anhydrous acetonitrile) in the presence of TFA (50 equiv, 250 mM). The concentration of (−)-cytidine was varied from 0 to 75 mM. DCLs were allowed to sit for more than 1 month, during which equilibrium was reached, and then analyzed by HPLC, monitoring the hydrazone absorption at 289 nm. Assuming that extinction coefficients in the UV trace (the hydrazone absorption at 289 nm) were equal for all oligomers regardless of their structures, the concentration of each oligomer in a DCL was produced by the following equation: 5 mM (monomer concentration) × HPLC-UV trace integrations of the oligomer as fractions of the total/number of monomer units in the oligomer (e.g., the number of monomer units is 2 in a dimer). Experiments were performed at least in duplicate, and the average values were used for simulations (see Supporting Information (SI) Table 1).

Numerical Simulations. The computational studies were performed with the help of the program Gepasi (v. 3.30).[9] The oligomer distribution of the DCL without (−)-cytidine template T was modeled by assuming fictitious equilibria between a monomer M and the respective oligomers MM, MMM, MMMM, and MMMMM (Scheme 1). The association constant K_{M2} was fixed arbitrarily at 10^8 M^{-1} (a high value was chosen to ensure a low final monomer concentration). The remaining association constants K_{M3}, K_{M4}, and K_{M5} were fitted to the equilibrium concentrations of the oligomers. The latter values were obtained by extrapolation of the oligomer distributions of (−)-cytidine-templated libraries to 0 mM template.

The association constants K_{M2}−K_{M5} were then fixed, and the model was expanded to include the interactions with the template (−)-cytidine (T). The interaction was described as a simple 1:1 complex with the binding constants K_{MXT} ($X = 2 - 5$). The equilibrium distributions were fitted to the concentrations, which were determined in experiments with a fixed monomer concentration of 5 mM and template concentrations ranging from 2.5 to 75 mM. It was assumed that the experimentally determined concentrations corresponded to the sum of the free and the complexed oligomers M*X* and M*X*T. For the fitting, a Levenberg−Marquardt algorithm was employed, followed by a second optimization with a Hooke and Jeeves algorithm (both are implemented in the Gepasi program). This procedure was found to provide fast and reliable fits to the data. To estimate the accuracy of the derived binding constants, the values of K_{M2T} [(*S*)-DCL] and K_{M4T} [(*R*)-DCL] were fixed at values that differed from the optimum values. The remaining three binding constants were then fitted to the experimental data, and the increased root-mean-square (rms) values were

(8) (a) Wagner, E. C.; Simons, J. K. *J. Chem. Educ.* **1936**, *13*, 265–272. (b) Ali, M. Y.; Dale, J.; Tilestad, K. *Acta Chem. Scand.* **1973**, *27*, 1509–1518. (c) Ali, M. Y.; Khatun, A. *Tetrahedron* **1985**, *41*, 451–454.

(9) (a) Mendes, P. *Comput. Appl. Biosci.* **1993**, *9*, 563–571. (b) Mendes, P. *Trends Biochem. Sci.* **1997**, *22*, 361–363.

noted. These data were used to generate a rms vs free energy of binding plot (see SI Figure 10).

HPLC-LP Analysis. A 10 μL DCL solution was injected and eluted through a C18 column (4.6 × 150 mm, 4.6 μm) at a flow rate of 1.0 mL/min. All separations were performed using gradient elutions of methanol/acetonitrile/water. To remove the solvent, TFA, and the template, 10% methanol/water for 3 min and then a linear gradient (10 to 40% methanol/water over 6 min) was used. A second gradient (10% acetonitrile/water for 5 min then increased to 43% acetonitrile/water over 17 min and steady 43% acetonitrile/water for more 2 min) was subsequently used to separate the library. This convoluted procedure removed traces of solvent and the template which adversely affected the LP baseline.

ESI-MS Analysis. ESI mass spectra were obtained using a Micromass ZQ mass spectrometer in positive ion mode with the ESI source. The DCLs (5 mM) were directly infused at a flow rate of 10 μL/min into the ion source. ESI-MS conditions were optimized to favor the observation of noncovalent intact host−guest complexes: 2.7 kV capillary voltage, 50 V cone voltage, 150 °C source temperature, 350 °C desolvation gas temperature, and 250 L/h desolvation gas (N_2) flow rate. Data were collected and analyzed using the MassLynx software, and 70−90 scans over the mass range of 150−1850 *m/z* were summed to obtain the final spectra in continuum mode.

Nanoflow Electrospray Ionization CID-MS/MS Analysis. Collision-induced dissociation (CID) measurements were performed on a hybrid quadrupole time-of-flight (Micromass Q-TOF micro) instrument (Waters, Manchester, UK). The instrument was equipped with a Z-nanoelectrospray source (Waters-Micromass) operated in a positive ionization mode. Uncoated fused-silica PicoTip emitters (New Objective) were used for nanoelectrospray, with capillary inner and outer diameters of 20 μm and 360 μm, respectively, pulled to a 10 μm inner diameter tip. The potential between the nanospray needle and the orifice of the mass spectrometer was set to 2.0 kV, with a cone voltage of 200 V. The samples were infused at a flow rate of 350 nL/min. For MS scans, the quadrupole was set to pass all ions, and a mass spectrum was generated by summing 120 scans over the mass range of 450−1600 *m/z*. The collision cell energy was set to 7 eV to decrease dissociation of noncovalent interactions. In MS/MS mode, the quadrupole was set to select for a single precursor ion, which was dissociated in the hexapole collision cell, generating product ions that were then mass analyzed by the time-of-flight mass analyzer. Argon gas was used as the collision gas in CID-MS/MS measurements. The collision cell voltage was varied from 10 to 70 eV for 1-min intervals with a scan time of 1 s and an interscan delay of 0.1 s. A mass spectrum was generated by averaging scans over 1 min. The intensities of the parent and product ions for each collision energy voltage interval were recorded. Since the work was primarily concerned with the dissociation of a noncovalent complex, the product ions of interest were limited to the host compound and its cytidine adduct. In continuum mode, for an ion intensity to be considered, a minimum of four scans per peak must be present. The percent intact complex was calculated by a ratio of the ion intensities (I) of the host−guest complex $[\text{host}\cdot\text{guest}]^+$, the resulting enantiomeric host, and the guest (either (−)-cytidine or (−)-2-thiocytidine): % Intact complex = $I_{[\text{host}\cdot\text{guest}]^+}/\{I_{[\text{host}\cdot\text{guest}]^+} + (I_{[\text{host}]^+} + I_{[\text{guest}]^+})/2\}$. The calculated percent intact complex was plotted as a function of the collision energy, and an E_{cm50} value was calculated by fitting the dissociation curve to a three-parameter sigmoidal function using SigmaPlot 9.0.[10] The E_{cm50} value represented the collision energy whereby 50% of the noncovalent complex became dissociated. Experiments were performed in triplicate, and the average percent intact complex values were depicted with standard deviations of <3. Error values were calculated on the basis of the relative uncertainties of each term in the average sigmoidal regression equation.

Scheme 2. Templating a (*rac*)-**1** DCL with (−)-Cytidine and (−)-2-Thiocytidine

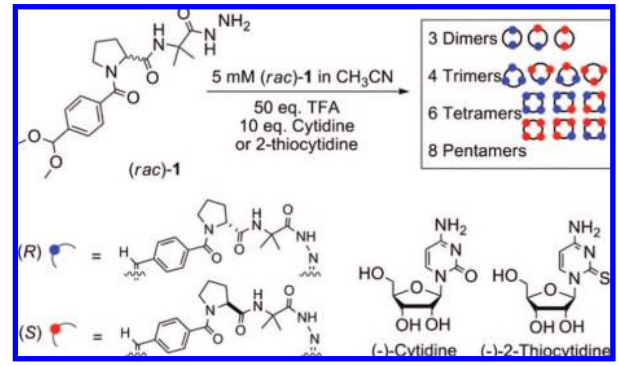

Results and Discussion

1. Library Generation and HPLC Analysis in Combination with Laser Polarimetry (LP). A mixture of the cyclic oligomers of (*rac*)-**1** was obtained by treating a solution of the protected monomer with TFA (Scheme 2): cyclic dimers, trimers, tetramers, and pentamers were observed, with the most abundant species being trimers (Figure 1b). Since the monomer was racemic, the library components were either achiral (*meso*) or racemic, and the ensemble was thus optically inactive. Consequently, each peak in the chromatogram did not rotate plane-polarized light, and the laser polarimeter detector trace was flat (Figure 1a). Using HPLC, diastereomer resolution was achieved for the dimer but not for the trimer and tetramer (partial) (Figure 1b).

When the DCL was templated with (−)-adenosine (10 equiv with respect to (*rac*)-**1**), the homodimers and the tetramers were amplified at the expense of the other oligomers (Figure 1d), with the changes being quantified by HPLC/UV (see boxed sections of Figure 1d). At equilibrium, the increase in the homodimers ($\Delta = +15\%$) and tetramers ($\Delta = +7\%$) implied that (−)-adenosine had a modest binding affinity to each of these receptors. The LP trace, however, showed that only the dimer had one of its enantiomers selectively amplified (*SS* from the sign of the rotation, Figure 1c inset), the flat line indicated that the amplified tetramer's enantiomers were either equally enhanced or too tiny to detect by the LP detector.[11] From a mass-balance perspective, the excess (*R*)-monomer was distributed into the other components of the DCL, though it appeared to be without any significant pooling and/or the (*R*)-rich species have low molar rotations.

When the DCL was instead templated with (−)-cytidine (10 equiv with respect to (*rac*)-**1**), the homodimers and tetramers were again amplified at the expense of trimers and pentamers (Figure 1f), but this time the LP showed peaks in the dimer, trimer, and tetramer regions. The magnitude of the increases

(10) The center-of-mass collision energy (E_{cm}) represents the maximum amount of kinetic energy that can be converted into internal energy upon collision activation under single-collision conditions. E_{cm} was obtained from $E_{\text{cm}} = E_{\text{lab}}[m_g/(m_g + m_p)]$, where E_{lab} is the laboratory frame kinetic energy or the charge (ze) multiplied by the potential difference between the collision and source regions (V), m_g the mass of the argon target gas, and m_p the mass of the parent ion. Although the collision event taking place in a quadrupole time-of-flight instrument actually consists of multiple collision events, E_{cm} provides a rudimentary basis for semiquantitative comparison. See footnote 20.

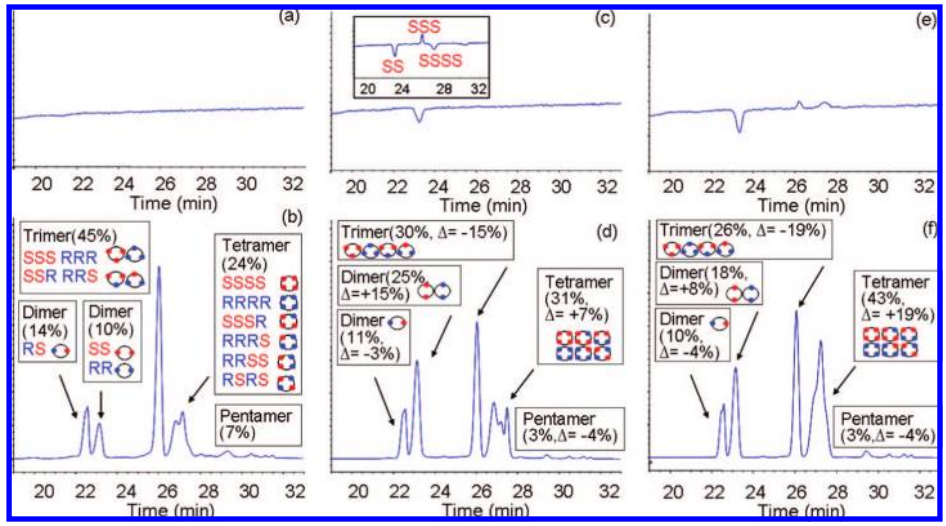

Figure 1. HPLC analysis (day 30) of untemplated (5 mM (*rac*)-**1**) and templated (5 mM (*rac*)-**1**, 50 mM (−)-adenosine, or 50 mM (−)-cytidine) samples in acetonitrile: (a) LP and (b) UV trace (289 nm) of untemplated DCL; (c) LP of DCL + (−)-adenosine [inset: LP of untemplated (*S*)-DCL (5 mM (*S*)-**1**)]; (d) UV (289 nm) of DCL + (−)-adenosine; (e) LP of DCL + (−)-cytidine; (f) UV (289 nm) of DCL + (−)-cytidine. The *y*-axes for panels (a)/(c)/(e) and (b)/(d)/(f) are normalized rotation and absorbance, respectively, and the Δ values were calculated from UV % areas.

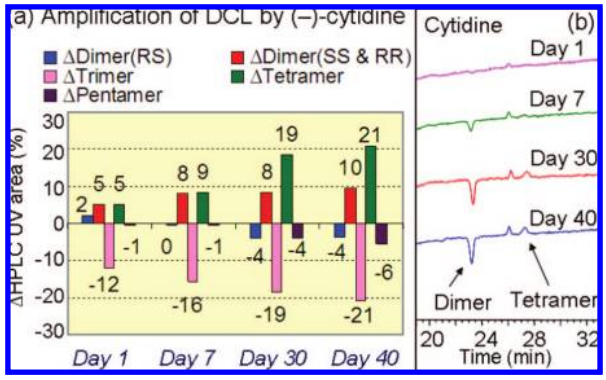

Figure 2. Time-dependent speciation and LP signals for (*rac*)-**1** + (−)-cytidine: (a) % UV area changes and (b) the associated LP traces for 5 mM (*rac*)-**1** and 50 mM (−)-cytidine in acetonitrile.

for the homodimers and tetramers (Δ = +8% and +19%, respectively) suggested modest binding affinities. Informative were the phases of the respective LP signals (Figure 1e). From the (*S*)-DCL (from (*S*)-**1**, Figure 1c inset), it was clear that (*SS*)-dimer was in excess. The opposite phase of the templated tetramer (cf. *SSSS* in Figure 1c inset) therefore indicated that the amplified tetramers were (*R*)-rich (*RRRR* and/or *RRRS*). (−)-2-Thiocytidine generated a similar amplification (Δ = +6% and +21%) and LP signal for the homodimer and tetramers (for details, see SI Figure 1); in general, the 2-thia congener behaved similar to (−)-cytidine.

When the evolution of the (−)-cytidine-templated DCL was monitored, it was noted that the tetramer concentration increased slowly but steadily over the time course (40 days), while the homodimer stabilized at or near a steady-state concentration after 7 days (Figure 2a).[12] The magnitude of the dimer's LP signal, however, continuously increased beyond the initial 7 days, when its concentration (by UV) had stabilized. By contrast, the LP signal of the tetramer increased steadily as its concentration increased (Figure 2b). These observations, along with selective losses in trimer and pentamer, suggested two possible scenarios: (1) the equilibrium was being driven by strong binding to an (*R*)-rich tetramer, which by mass action caused a sympathetic enhancement in (*SS*)-dimer, or (2) the equilibrium was being driven by enantioselective binding to *both* the (*R*)-rich tetramer and the (*SS*)-dimer. Regardless of the cause, it was clear that the template was causing the (*R*)- and (*S*)-components of the library to partition into the (*SS*)-dimer and an (*R*)-rich tetramer, i.e., become deracemized.

2. Pseudo-enantiomers for LC-MS Diastereomer Determination and Quantitation. To quantify the enantioenrichment of (*SS*)-dimer and the (*R*)-rich tetramers, a pseudo-racemic monomer pair was utilized,[5] wherein mass-tagged enantiomers were combined to uniquely identify each possible diastereomer by mass spectrometry. The mass-tagging was accomplished by preparing (*S*)-**1**-d_6 (from α-methylalanine-d_6[8]) and mixing it with (*R*)-**1**. UPLC-MS analysis of the untemplated DCL indicated that the statistically favored heterochiral structures were dominant (Table 1).[13] (−)-Cytidine, however, shifted the speciation from heterochiral to homochiral structures. The thermodynamic selectivity of the dimers, as measured by the equilibrium ratio of (*SS*)-d_{12}- to (*RR*)-dimer increased to 3.0:1 (50% ee).[14] In the tetramers, the *SRRR*-d_6-to-*RSSS* ratio was nearly 1:1, while the (*RRRR*)-to-(*SSSS*)-d_{24} tetramer ratio increased to 5.6:1 (68% ee). The *deamplified* trimer was significantly perturbed from racemic as the (*SSR*)- and (*SSS*)-diastereomers were enhanced to 31% and 68% ee, respectively (Table 1).

The (−)-2-thiocytidine template behaved similarly, with the homochiral dimer, trimer, and tetramer being perturbed to 58%, 71%, and 69% ee, respectively (Table 1). In addition to

(11) These results were obtained using different reaction conditions (solvent, monomer, and guest concentration) from our previously reported results using (*rac*)-**1** DCL (see ref 5).

(12) After 40 days, the untemplated DCL degrades, making it impossible to directly compare the two samples beyond this time. The (−)-cytidine-templated DCL maintains its integrity beyond several months.

(13) These measurements were obtained in the selective mass range ion chromatogram and integrated over the eluting peak in question. Erroneous results were obtained using the total ion chromatogram: Schiltz, H., Chung, M.-K., Gagné, M. R. *Org. Biomol. Chem.* **2008**, DOI:10.1039/b80849d.

(14) In contrast, (−)-adenosine was significantly less enantioselective under the present conditions. The dimer was obtained in 22% ee (UPLC-MS analysis).

Table 1. Equilibrium Dimer, Trimer, and Tetramer Diastereo Compositions from UPLC-MS Analysis on a 1:1 Mixture of (*S*)-**1**-d_6 and (*R*)-**1**[a]

	untemplated (%)[b]	cytidine-templated (%)[c]	2′-thiocytidine-templated (%)[d]
dimer (*SS*)-d_{12}:(*RS*)-d_6:(*RR*)	21:57:21	51:33:17	51:35:14
trimer (*SSS*-d_{18}):(*SSR*-d_{12}):(*SRR*-d_6):(*RRR*)	9:42:42:8	22:48:26:4	23:51:23:4
tetramer (*SSSS*-d_{24}):(*SSSR*-d_{18}):(*SSRR*-d_{12}):(*SRRR*-d_6):(*RRRR*)	15:22:25:24:14	9:14:14:13:50	10:11:13:11:54
	Enantiomeric Excess (%)		
dimer (*SS* to *RR*)		50 ± 0.7	58 ± 0.0
trimer (*SSS* to *RRR*; *SSR* to *RRS*)		68 ± 2.7; 31 ± 2.1	71 ± 0.9; 38 ± 0.2
tetramer (*RRRR* to *SSSS*)		68 ± 1.1	69 ± 1.7

[a] These measurements were taken in a selection mode on the peak in question. Total ion chromatograms gave erroneous results (see footnote 13). [b] Average of six separately prepared samples (days 7−14). Standard deviation of average compositions, ±0.3−0.8%. [c] Average of three separately prepared samples. Standard deviation of average compositions, ±0.2−1.0%. [d] Average of two separately prepared samples. Standard deviation of average compositions, ±0.1−1.1%.

measuring the ratio of stereoisomers, this analysis unambiguously identified *RRRR* as the amplified tetramer that generated the LP signal in Figures 1e and 2b. The positively phased trimer peak in Figure 1e thus reflected a weighted (by their specific rotations) sum of the *SSS* and *SSR* excesses.

To confirm these results and rule out the possibility of the ESI process affecting the quantitation of the oligomers, we sought an independent means of measuring the enantioselectivity. This was accomplished on the dimer by a combination of HPLC/LP and UV analyses. Since the LP signal is a differential enantiomeric concentration,[15] several mixtures of (*R*)-**1** and (*S*)-**1**-d_6 were combined to calibrate this signal to the total dimer concentration (HPLC/UV). One curious complication emerged from the slightly different retention times for (*RR*)- and (*SS*)-d_{12}-dimers, which caused the LP traces to be sigmoidal. The differential area of the homodimers was therefore obtained by adding the two oppositely phased LP areas (SI Figure 2). The calibration curve shown in SI Figure 3 enabled the synthetic mixtures to be analyzed and compared by the two methods (SI Table 2). The agreement was excellent, and so several templated systems were compared (SI Table 3); the results were of equally high quality. These validation results of the more convenient UPLC-MS method indicated no detrimental ESI artifacts in the dimers.[13]

For cyclic tetramers, incomplete diastereomer resolution in the HPLC did not allow a similar direct comparison. However, the resolution power of UPLC (Waters) and rapid-resolution LC (Agilent) provided better diastereomer resolution and a more refined analysis (SI Figure 4). The UPLC/UV and rapid-resolution LC/UV analyses provided relative concentrations of (*RRSS* + *RSRS*) to the rest of tetramers, and ratios of (*RRRS* + *SSSR*) to (*RRRR* + *RRSS* + *RSRS* + *SSSS*), respectively (SI Tables 4 and 5). The similarity of these same ratios, calculated directly from the MS compositions, again suggested that diastereomer analysis by UPLC-MS was accurate.[13] A third validation of the UPLC-MS approach was obtained by noting that the (*SRRR*)-d_6-tetramer:(*SSSR*)-d_{18} ratio was nearly 1 in UPLC-MS analysis, suggesting that the LP area of the tetramers should directly correlate to the differential homotetramer concentrations. From a calibration curve relating LP area and homotetramer concentrations (SI Figure 5), the differential concentration of homotetramers ([*RRRR*] − [*SSSS*]) in several templated DCLs was obtained and compared to the direct

(15) Since optical rotation is affected by temperature, wavelength, solvent, and pH, these four parameters were fixed during the optical rotation measurements.

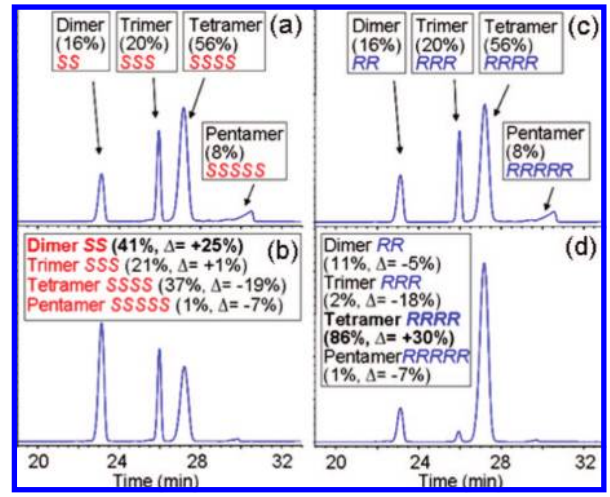

Figure 3. Equilibrium HPLC/UV traces (289 nm) for 5 mM DCLs: (a) untemplated (*S*)-**1**; (b) (*S*)-**1** + (−)-cytidine (50 mM); (c) untemplated (*R*)-**1**; (d) (*R*)-**1** + cytidine (50 mM). Δ = % $\text{oligomer}_{\text{templated}}$ − % $\text{oligomer}_{\text{untemplated}}$.

UPLC-MS measurements (SI Table 6). The similarity of the two analyses again confirmed the accuracy of the UPLC-MS measurements.

3. Templating of Enantiopure DCLs with (−)-Cytidine and (−)-2-Thiocytidine. The amplification of *SS* and *RRRR* in the templated (*rac*)-DCLs suggested good binding affinities between these species and (−)-cytidine and (−)-2-thiocytidine. To support this supposition, (−)-cytidine and (−)-2-thiocytidine were each used to template an (*S*)-**1** and an (*R*)-**1** DCL. As expected, (−)-cytidine amplified the dimer (Δ = +25%) in the (*S*)-DCL (Figure 3b) and the tetramer in the enantiomeric (*R*)-DCL (86% of total, Δ = +30%, Figure 3d). Again, (−)-2-thiocytidine behaved similarly (SI Figure 6).

As shown in Figure 4, the evolution of the two libraries was monitored over time, and it was observed that the dimer-favored (*S*)-library came to equilibrium faster than the tetramer-favored (*R*)-library. Apparently, tetramers grew more slowly than dimers. From the equilibrium speciation, both templated and untemplated, it could be deduced that the binding constants for (−)-cytidine ranked in the order $K_{SS} > K_{SSS} > K_{SSSS}$ for the (*S*)-DCL and $K_{RRRR} > K_{RR} > K_{RRR}$ for the (*R*)-DCL.

4. ESI-MS Analysis of Templated DCLs. To the extent that gas-phase effects could be correlated to solution results, we sought to address questions of diastereomeric binding affinity in ESI-MS of active templating solutions by looking for intact

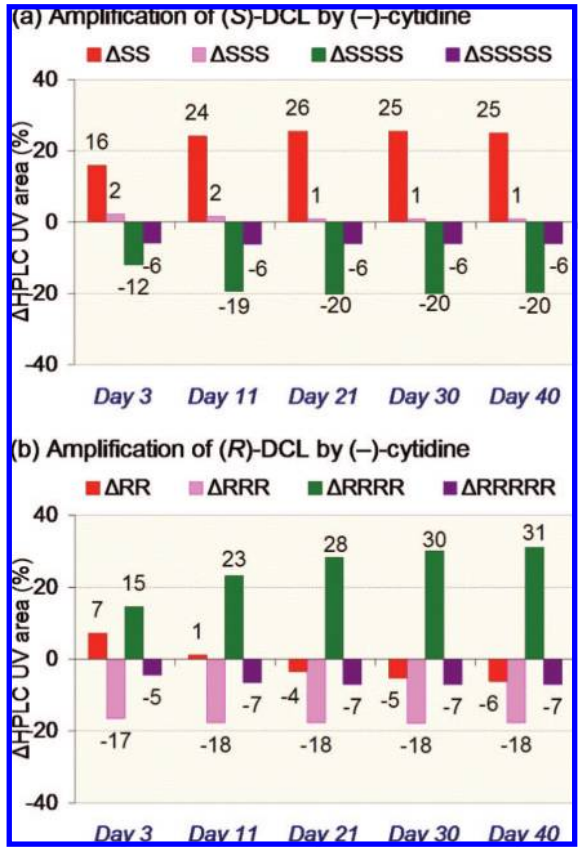

Figure 4. Time-dependent speciation (Δ = % oligomer$_{templated}$ − % oligomer$_{untemplated}$). Due to long-term degradation of untemplated DCLs, % oligomer$_{untemplated}$ was obtained at day 11: (a) 50 mM (−)-cytidine + 5 mM (*S*)-**1**; (b) 5 mM (*R*)-**1** + 50 mM (−)-cytidine.

host−guest ions. The intensity of intact host−guest adducts in ESI-MS has previously been used to estimate the relative binding affinities of noncovalent host−guest pairs.[16,17] Since the mass-tagged libraries were diastereo-resolved, we hoped that (−)-cytidine-templated DCLs would be similarly informative. As expected for the untemplated DCL, [dimer·H]$^+$, [trimer·H]$^+$, [tetramer·H]$^+$, and [pentamer·H]$^+$ were observed, with each of the diastereomers identifiable by its unique molecular weight (Figure 5a). For (−)-cytidine-containing DCL solutions, the hosts and their respective 1:1 host−guest ions were observed for nearly all of the oligomers (except pentamers), though the intensities of the individual adducts were variable and sensitive to spectrometer settings (Figure 5b). The host−guest adducts of the pentamer extended beyond the mass range of our instrument. Additionally, a small amount of the [dimer·2cytidine·H]$^+$ ion was detected.

The observation that nearly every cyclic host formed a detectable adduct with [cytidine·H]$^+$ suggested a finite binding affinity to each guest, where previous ESI mass spectra of peptide-based hydrazone host−guest solutions have been dominated by a specific host−guest adduct.[17] Even when substoichiometric quantities of (−)-cytidine (0.16 equiv) were utilized, ESI-MS revealed adducts between all oligomers and the template.

To test whether the templating selectivity was detectable in the ESI-MS, a library sample was combined with 0.16 equiv of (−)-cytidine. Under these conditions, nonsaturation should allow the analyte to choose from the mixture of (mostly static) diastereomeric receptors with a preference correlated with its

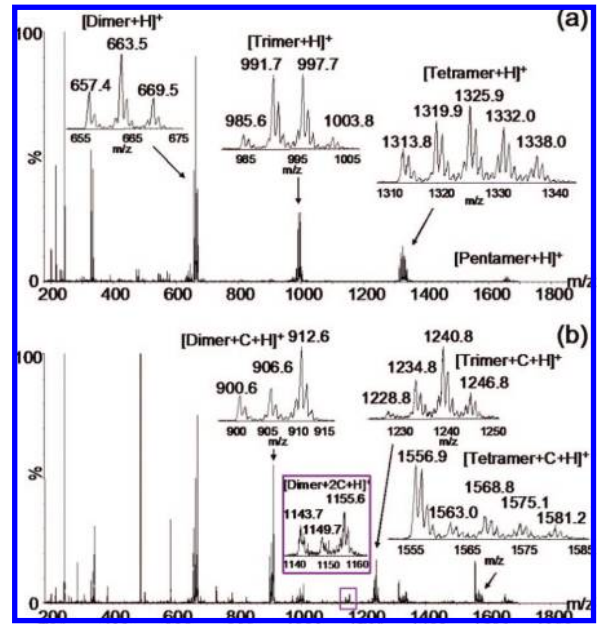

Figure 5. ESI-MS spectrum of (a) untemplated DCL (5 mM, (*S*)-**1**-d_6:(*R*)-**1** = 1:1); (b) (−)-cytidine-templated DCL (5 mM, (*S*)-**1**-d_6:(*R*)-**1** = 1:1, 250 mM cytidine).

inherent binding preference (a thermodynamically controlled scenario). Under the experimental conditions, both [dimer·H]$^+$ and [dimer·cytidine·H]$^+$ were well populated, and the dr's of the free receptor mirrored the nontemplated situation (*RR*:*RS*:*SS* = 26:50:24), while the host−guest ion was perturbed toward the better binding dimer (i.e., *RR*:*RS*:*SS* = 24:41:34, Figure 6). Although the quantitative parallels to a solution DCC experiment are unclear, the (*SS*)-dimer was enhanced in both circumstances; (−)-thiocytidine behaved similarly (SI Figure 7).

In contrast to the preference observed in the dimer, the tetramer showed only a marginal change in the ratio of host−guest ions from the background ratio of 12:26:29:23:10 (*RRRR*:*RSSS*:*RRSS*:*RSSS*:*SSSS*). In the cytidine-templated DCL, the ratios were 10:25:34:23:9 (free tetramer) and 11:28:32:19:9 (cytidine adducts), respectively, and reflected a shift in the ratio of the hetero and meso species but not exclusively toward *RRRR*. This behavior was again mirrored in thiocytidine-templated DCLs (SI Figure 7). Whatever process was responsible for the dimer perturbation was inoperative, too weak, or too slow to influence ion generation in the homotetramers.[18]

5. Relative Stability Determination of Diastereomeric Adducts by CID-MS/MS. Another mass spectrometric approach for characterizing the host−guest assemblies was to measure

(16) ESI-MS applications (general): (a) Daniel, J. M.; Friess, S. D.; Rajagopalan, S.; Wendt, S.; Zenobi, R. *Int. J. Mass Spectrom.* **2002**, *216*, 1–27. (b) Gabelica, V.; De Pauw, E. *Int. J. Mass Spectrom.* **2002**, *219*, 151–159. (c) Schug, K.; Frycak, P.; Maier, N. M.; Lindner, W. *Anal. Chem.* **2005**, *77*, 3660–3670. (d) Rosu, F.; Pirotte, S.; De Pauw, E. *Int. J. Mass Spectrom.* **2006**, *253*, 156–171.

(17) ESI-MS applications (peptide-based hydrazone chemistry): (a) Poulsen, S.-A.; Gates, P. J.; Cousins, G. R. L.; Sanders, J. K. M. *Rapid Commun. Mass Spectrom.* **2000**, *14*, 44–48. (b) Cousins, G. R. L.; Furlon, R. L. E.; Ng, Y.-F.; Redman, J. E.; Sanders, J. K. M. *Angew. Chem., Int. Ed.* **2001**, *40*, 423–428. (c) Lam, R. T. S.; Belenguer, A.; Roberts, S. L.; Naumann, C.; Jarrosson, T.; Otto, S.; Sanders, J. K. M. *Science* **2005**, *308*, 667–669. (d) Liu, J. Y.; West, K. R.; Bondy, C. R.; Sanders, J. K. M. *Org. Biomol. Chem.* **2007**, *5*, 778–786.

(18) Arguing against a concentration-dependent phenomenon were experiments with progressively more dilute injection solutions, which did not lead to significant differences in the diastereomeric ratios of host−guest adducts relative to the free [host·H]$^+$ ions.

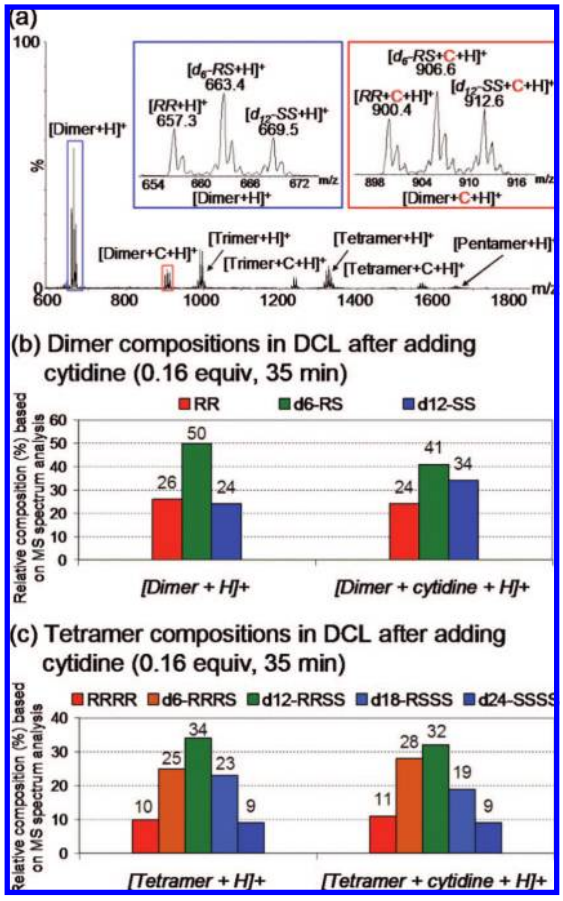

Figure 6. (a) ESI mass spectrum of a DCL 35 min after adding (−)-cytidine (0.16 equiv, 0.8 mM). Panels (b) and (c) represent the diastereo-speciation of dimers and tetramers and their corresponding host−guest complexes.

the binding strength of the adducts by tandem mass spectrometry (MS/MS) in combination with collision-induced dissociation (CID).[19] Since a noncovalent host−guest ion should first break down to guest and host, this fragmentation should be modulated by the applied collision energy. Since each diastereomer had a unique mass, the energy dependence of the fragmentation could be measured for each diastereomer.[20]

The CID mass spectra for the MS-selected ion ([(*SS*)-d_{12}-dimer·cytidine·H]$^+$, m/z = 912.4) is shown in Figure 7. At low collision voltages, the parent ion remained intact. As the collision energy was increased, the host−guest ion began to fragment first to host ([(*SS*)-d_{12}-dimer·H]$^+$, m/z = 669.3) and then eventually to [cytidine·H]+ and [((*SS*)-d_{12}-dimer)/2·H]$^+$ at high potentials. Plots of the percentage of intact host−guest adduct versus the center-of-mass collision energy (eV)[10] provided reliable and reproducible measures of the energy needed to exactly reduce the parent ion to 50% of its original intensity (E_{cm50}, Figure 8).[16,21] The [(*RR*)-dimer·cytidine·H]$^+$ ion was also selected and subjected to the CID sequence of

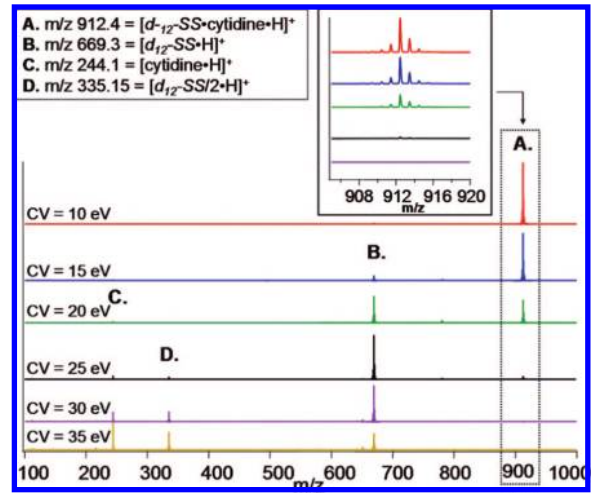

Figure 7. CID-MS/MS spectra of [*SS*-d_{12}·cytidine·H]$^+$ (marked A) at various collision cell voltages. The B, C, and D ions are the expected host, guest, and fragmented host, respectively.

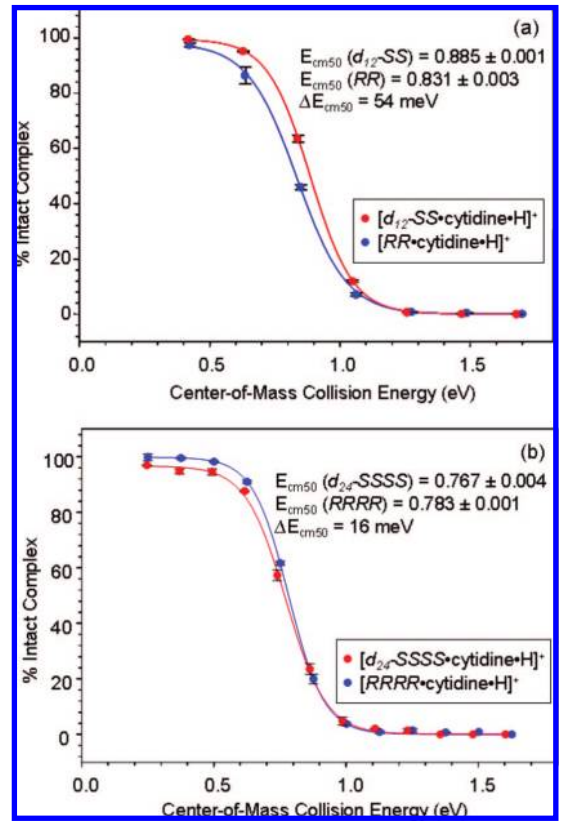

Figure 8. Dissociation curves of the dimer- and tetramer-derived intact complexes: (a) [*SS*-d_{12}·cytidine·H]$^+$ and [*RR*·cytidine·H]$^+$, (b) [*SSSS*-d_{24}·cytidine·H]+ and [·cytidine·H]$^+$. The intact complexes were generated in (−)-cytidine-templated DCL ((*R*)-**1**:(*S*)-**1**-d_6 = 1:1). The % of intact complex was calculated using the equation, % Intact complex = $I_{[host\cdot guest]^+}$/{$I_{[host\cdot guest]^+}$ + ($I_{[host]^+}$ + $I_{[guest]^+}$)/2}, where *I* represents the ion intensity, host is the enantiomeric dimers and tetramers, and guest is cytidine.

measurements. As shown in Figure 8a, the dissociation curve for the (*SS*)-d_{12}-diastereomer was shifted to higher energy (by

(19) (a) Czerwenka, C.; Linder, W. *Rapid Commun. Mass Spectrom.* **2004**, *18*, 2713–2718. (b) Catalina, M. I.; de Mol, N. J.; Fischer, M. J. E.; Heck, A. J. R. *Phys. Chem. Chem. Phys.* **2004**, *6*, 2572–2579. (c) Filippi, A.; Gasparrini, F.; Pierini, M.; Speranza, M. *J. Am. Chem. Soc.* **2005**, *127*, 11912–11913.

(20) Each enantiomeric host−guest pair follows an identical fragmentation pathway, allowing for comparison of their relative binding strengths. However, since the fragmentation may also be influenced by heightened internal energy from an increased cone voltage during the transfer of desolvated ions to the mass analyzer, dimer and tetramer dissociation energies are not comparable.

(21) (a) Giorgio, G.; Speranza, M. *Int. J. Mass Spectrom.* **2006**, *249−250*, 116–119. (b) Jorgensen, T. J. D.; Delforge, D.; Remacle, J.; Bojesen, G.; Roepstorff, P. *Int. J. Mass Spectrom.* **1999**, *188*, 63–65. (c) Li, H.; Zhou, J.; Yuan, G. *J. Am. Soc. Mass Spectrom.* **2005**, *17*, 9–14.

54 meV), indicating that it bound (−)-cytidine more strongly than did the (*RR*)-receptor.

The tetrameric host−guest adducts were similarly analyzed, and it was found that *RRRR* bound to (−)-cytidine more strongly than *SSSS*-d_{24} by 16 meV (Figure 8b). To reduce the measurement errors, the same ions were selected from DCL samples prepared from a 1:2 ratio of (*R*)-**1** and (*S*)-**1**-d_6, as these contained higher concentrations of *SSSS*-d_{24}-; the data were found to be highly reproducible (SI Figure 8). As consistently observed in the above characterization methods, (−)-2-thiocytidine paralleled (−)-cytidine. In this case, *RR*- and *SSSS*-d_{24} bound (−)-thiocytidine 46 and 55 meV more strongly than their enantiomeric counterparts (SI Figure 9a,b).

Fragmentation ratios (R) could also be calculated at collision cell energies (E_{lab}), where the fragmentation was dominated by simple host−guest dissociation (see Figure 7).[22] For the two diastereomers (at E_{lab} = 20 and 30 eV for dimer and tetramer, respectively), the extent of fragmentation could be compared by the ratio of the individual *R*'s (SI Table 7). These alternative measures of binding strength indicated that, at a similar collision energy, (*SS*)- fragmented less than (*RR*)-dimer (R_{RR}/R_{SS} = 1.9 at 20 eV), while *RRRR* was similarly more stable than *SSSS* (R_{SSSS}/R_{RRRR} = 1.3 at 30 eV). The (−)-thiocytidine-templated experiments gave R_{RR}/R_{SS} = 1.8 at 20 eV and R_{SSSS}/R_{RRRR} = 1.7 at 30 eV. To the extent that gas-phase dissociation energies correlate with solution binding constants,[23] these data show that both the dimer and the tetramer have an enantiomer preference in their respective host−guest adducts and are thus consistent with scenario 1 in section 1, where both the (*SS*)- and the (*RRRR*)-receptors act in concert to deracemize the library.

6. Host−Guest Binding Affinities by Numerical Simulations. Numerical simulations are a valuable tool for studying the adaptive behavior of DCLs.[24] Recently, it has been shown that simulations in combination with fitting procedures can also be used to derive binding constants from species distributions.[25] This method thus represents a powerful alternative for determining binding constants of systems, where it is not possible to investigate the host properties of isolated library members.[26]

Our computational studies focused on the enantiopure (*S*)- and (*R*)-DCLs, reasoning that, since the principal receptors were homochiral in nature, their simulation might provide helpful insights for explaining the deracemization trends. To this end, we collected equilibrium concentration data for the dimer, trimer, tetramer, and pentamer (monomer concentration = 5 mM) as a function of (−)-cytidine concentration (2.5−75 mM).[27] Oligomer concentrations were obtained from the HPLC/UV trace, assuming that ϵ_{289nm} scaled with the number of monomer units in the structure. The resulting data were fitted to a simple model, which assumed that every library member could form a 1:1 complex with the template (see details in the Experimental Section). The fitting was performed with the help of the program Gepasi (v. 3.30),[9] which computes error-minimized binding constants for each of the oligomers. Good fits were obtained between the simulated DCLs and the experimental data (Figure 9).[28,29]

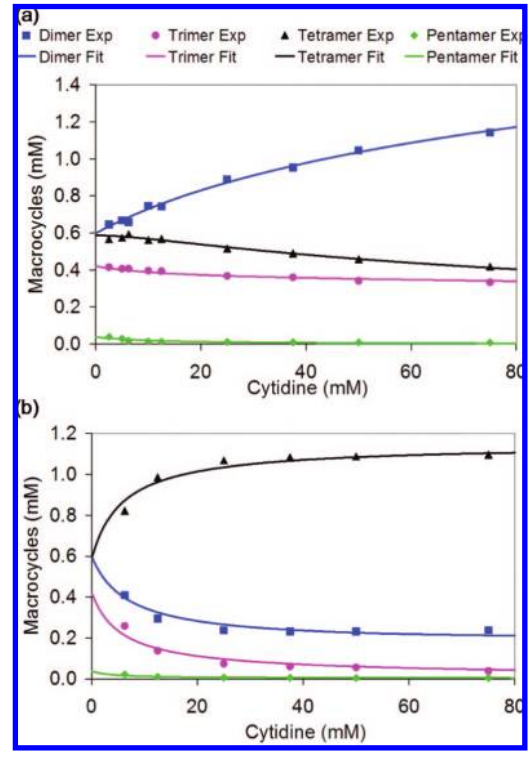

Figure 9. Best-fit (−)-cytidine-templated enantiopure DCLs: (a) (*S*)-DCL (rms, 0.5460%) and (b) (*R*)-DCL (rms, 0.8551%). Points represent the experimental data, and lines represent the fit of simulated DCLs.

The computed binding constants and the corresponding free energies are listed in Table 2. It can been seen that the (*S*)- and the (*R*)-DCLs gave very different results. For the (*S*)-library, the dimer, trimer, and tetramer were found to be nearly equal receptors for (−)-cytidine (binding energy, 10−11 kJ/mol). Interestingly, the binding affinity of the (*SSSS*)-tetramer (−11.0 kJ/mol) was slightly larger than that of the (*SS*)-dimer (−9.8 kJ/mol), although it was dimer that was amplified at the expense of tetramer (Figure 3b). The breakdown in the correlation

(22) These E_{lab} values were slightly lower than E_{lab50} for each diastereomer.
(23) While the gas-phase stability of a host−guest pair that relies on solvent-dependent hydrophobic interactions can be very different from that in the solution phase, systems reliant on electrostatic and hydrogen-bonding interactions are generally more similar to the solution phase upon electospray transfer: (a) Hofstadler, S. A.; Griffey, R. H. *Chem. Rev.* **2001**, *101*, 377–390. (b) Schalley, C. A.; Castellano, R. K.; Brody, M. S.; Rudkevich, D. M.; Siuzdak, G.; Rebek, J., Jr. *J. Am. Chem. Soc.* **1999**, *121*, 4568–4579. (c) Wu, Q.; Gao, J.; Joseph-McCarthy, D.; Sigal, G. B.; Bruce, J. E.; Whitesides, G. M.; Smith, R. D. *J. Am. Chem. Soc.* **1997**, *119*, 1157–1158. (d) Robinson, C. V.; Chung, E. W.; Kragelind, B. B.; Knudsen, J.; Aplin, R. T.; Poulsen, F.; Dobson, C. R. *J. Am. Chem. Soc.* **1996**, *118*, 8646–8653.
(24) (a) Corbett, P. T.; Sanders, J. K. M.; Otto, S. *Chem.-Eur. J.* **2008**, *14*, 2153–2166. (b) Corbett, P. T.; Sanders, J. K. M.; Otto, S. *Angew. Chem., Int. Ed.* **2007**, *46*, 8858–8861. (c) Corbett, P. T.; Sanders, J. K. M.; Otto, S. *J. Am. Chem. Soc.* **2005**, *127*, 9390–9392. (d) Severin, K. *Chem. Eur. J.* **2004**, *10*, 2565–2580. (e) Corbett, P. T.; Otto, S.; Sanders, J. K. M. *Org. Lett.* **2004**, *6*, 1825–1827. (f) Corbett, P. T.; Otto, S.; Sanders, J. K. M. *Chem. Eur. J.* **2004**, *10*, 3139–3143. (g) Grote, Z.; Scopelliti, R.; Severin, K. *Angew. Chem., Int. Ed.* **2003**, *42*, 3821–3825.
(25) Ludlow, R. F.; Liu, J.; Li, H.; Roberts, S. L.; Sanders, J. K. M.; Otto, S. *Angew. Chem., Int. Ed.* **2007**, *46*, 5762–5764.
(26) As the protonated (−)-cytidine and (−)-2-thiocytidine appear to be the actual templates, the investigation of the host binding properties requires acidic conditions under which the host will re-equilibrate. See refs 3 and 5.
(27) See SI Table 1 for data compilation.
(28) Due to library degradation occuring faster than equilibration (at [cytidine] = 0), these data were not used in the simulations. Library equilibration times were found to increase with decreasing concentrations of cytidine.
(29) As pointed out by an insightful reviewer, the phenomenon discussed in the previous footnote is a mechanism whereby an external decomposition force could act on a templated library to magnify chirality, through either chiral host−guest attenuation or acceleration of the decomposition.

Table 2. Binding Constants K and Gibbs Free Energies ΔG° for Binding of Oligomers in (*S*)-/(*R*)-DCLs to (−)-Cytidine

(*S*)-DCL			(*R*)-DCL			
oligomer	K (M^{-1})[a]	ΔG° (kJ·mol^{-1})[a]	oligomer	K (M^{-1})[a]	ΔG° (kJ·mol^{-1})[a]	$\Delta\Delta G^\circ$ ($S - R$) (kJ·mol^{-1})
SS	71	−10.6	*RR*	7.6	−5.0	−5.6
SSS	51	−9.8	*RRR*	∼0	∼0	∼9.8
SSSS	86	−11.0	*RRRR*	481	−15.3	+4.3
SSSSS	−[b]	−[b]	*RRRRR*	60	−10.1	−

[a] At 25 °C. [b] The best fit to the data does not lead to a defined energy minimum (see SI Figure 10).

between amplification and binding affinity has been predicted theoretically;[24] however, only a few experimental studies have observed this behavior.[24a,c,30]

On the other hand, the (*R*)-DCL showed a clear delineation between the different receptors, with the tetramer binding strongest (−15.3 kJ/mol), followed by the pentamer (−10.1 kJ/mol) and the dimer (−5.0 kJ/mol) (Table 2). This was entirely consistent with the observation of strong tetramer amplification in Figure 3d (86% of total at equilibrium).

The relative binding constants for pairs of enantiomeric receptors showed that strong discrimination was indeed possible (Table 2). The difference between the (*SS*)- and the (*RR*)-receptor was 5.6 kJ/mol, while it was 4.3 kJ/mol for the tetramers. This suggested that the observed deracemization was a result of *RRRR* and *SS* each binding to (−)-cytidine with a significant enantioselectivity, which mutually enhanced their individual amplifications by partitioning their enantiomeric units into the competing manifold. The simulation data also explained why the trimer was formed enantioselectively, even though it was deamplified upon addition of (−)-cytidine (Figure 2a). Although *SSS* did not outcompete *SS*, its reasonable binding affinity would maintain a finite concentration under competitive pressures; *RRR*, on the other hand, was the poorest of the receptors.

Conclusions

High levels of enantioselectivity have been identified in the molecular recognition of (−)-cytidine and (−)-2-thiocytidine by hydrazone-based dipeptides. From a racemic library of components, the analytes amplify (*SS*)-dimer and (*RRRR*)-tetramer from a racemic state to levels of 50−58% ee and 68−69% ee, respectively. The enantio-divergent binding affinities of the (*RR*)-dimer and the (*RRRR*)-tetramer for (−)-cytidine clearly demonstrate the transition from molecular to supramolecular properties, each supramolecular whole being distinct from its constituents. In addition, the simulations revealed a special case wherein the amplification efficiency did not correlate with the strength of binding. The combination of LP detection and pseudo-enantiomer analysis provided a highly sensitive means for experimentally detecting and probing chiral solution-phase molecular recognition phenomena, while gas-phase ESI-MS and MS/MS analyses provided effective tools for evaluating the selection preference of these systems once they had been transported into the gas phase. The combination of these experimental techniques along with equilibrium simulations generated a picture of the observed deracemization that was best interpreted as being due to the amplification of an (*SS*)-receptor and an (*RRRR*)-receptor by the enantioselective binding to (−)-cytidine and (−)-2-thiocytidine. This behavior mutually enhances the degree of deracemization and lowers the energy of the coupled system.

Acknowledgment. M.R.G. and J.W.J. thank the Defense Threat Reduction Agency (DTRA) for support (W911NF06-1-0169), S.T.L. thanks the Army Research Office (W911NF04D0004), and K.S. thanks the Swiss National Science Foundation and the EPFL for kind support. We also acknowledge helpful discussions with Prof. Marcey Waters (UNC Chapel Hill).

Supporting Information Available: HPLC/UV-LP, UPLC-MS, rapid resolution LC-MS, ESI-MS, and CID-MS/MS analyses of (−)-2-thiocytidine-templated DCLs, various analyses of untemplated and (−)-cytidine-templated DCLs, HPLC UV area (%) and concentrations of oligomers for the simulation, and the best fits of simulated (−)-cytidine-templated DCLs. This material is available free of charge via the Internet at http://pubs.acs.org.

JA803658N

(30) Saur, I.; Severin, K. *Chem. Commun.* **2005**, 1471–1473.